# Hybrid Study of the Geophysical Situation in the Depressed Zone of Hydroelectric Power Plants Reservoir

Pavlo Anakhov[1], Viktoriia Zhebka[2], Vladislav Kravchenko[2], Pavlo Skladannyi[3], and Oleksii Zhyltsov[3]

[1] *National power company "Ukrenergo," 25 S. Petliuri str., Kyiv, 01032, Ukraine*
[2] *State University of Information and Communication Technologies, 7 Solomenskaya str., Kyiv, 03110, Ukraine*
[3] *Borys Grinchenko Kyiv University, 18/2 Bulvarno-Kudriavska str., Kyiv, 04053, Ukraine*

**Abstract**

The purpose of the study is to research the prospects of joint use of signals caused by standing waves of water bodies when studying the geophysical situation near hydroelectric power plants. The study is preceded by the development of recommendations for the protection of telecommunications. The main variables taken into account in the analysis of standing wave oscillations are considered in detail: amplitude of oscillations and their attenuation, period. The seismic-acoustic method of studying the geophysical situation in the depressive zone of a hydroelectric power station reservoir is modified by supplementing the hybrid seismic-acoustic signal with electromagnetic waves excited by microseismic oscillations. A generalized hybrid study of natural phenomena and anthropogenic events is reduced to the measurement and subsequent analysis of a hybrid signal that has more than one manifestation. Manifestations are determined by the number of signal transmission media, taking into account their physical nature.

**Keywords**

Geomagnetic storm, hybrid signal manifestation, microbaroms, microseism, physical domain of signals, transmission medium.



## 1. Introduction

The sphere of influence of the reservoirs of large Hydroelectric Power Plants (HPPs) involves colossal massifs of rocks. The complex of geophysical fields and processes, and mechanical and electrical transformations cause changes in the geophysical situation of the local environment in the depressed zone. This determines the need for a detailed study of the situation and makes specific recommendations for the protection of telecommunications near HPPs [1–2].

A significant factor of environmental impact is the field of microseismic oscillations excited by Standing Waves (SW) in a reservoir [3]. It has been determined that SW, in addition to microseisms, excites infrasound oscillations—microbaromics [3–4].

The addition of infrasound observations to microseismic data improves the efficiency of studying natural phenomena and man-made events [5–6].

For example, the analysis of seismic and acoustic signals allowed us to accurately determine the time of the eruption of the Stromboli volcano, in Italy [7]. The analysis of seismic-acoustic signals is also used to estimate the flow velocity and depth of mudflows in the Illgraben River catchment area, in Switzerland [8]. The joint analysis of infrasound and microseismic signals generated by explosions gives results that are correct in 85% of cases [9].

CPITS-2023-II: Cybersecurity Providing in Information and Telecommunication Systems, October 26, 2023, Kyiv, Ukraine
EMAIL: anakhov@i.ua (P. Anakhov); viktoria_zhebka@ukr.net (V. Zhebka); vladkr58@gmail.com (V. Kravchenko); p.skladannyi@kubg.edu.ua (P. Skladannyi); o.zhyltsov@kubg.edu.ua (O. Zhyltsov)
ORCID: 0000-0001-9169-8560 (P. Anakhov); 0000-0003-4051-1190 (V. Zhebka); 0000-0002-4758-7027 (V. Kravchenko); 0000-0002-7775-6039 (P. Skladannyi); 0000-0002-7253-5990 (O. Zhyltsov)

The mechanisms of energy conversion of microseismic oscillations are determined by electromagnetic radiation, which complements the complex impacts of reservoirs on the environment [1, 10–11].

The purpose of the study is to research the prospects for the joint use of microseisms, microbars caused by standing waves of water bodies, and electromagnetic waves excited by microseismic oscillations in the study of the geophysical situation near HPPs.

## 2. Oscillation Definition

Oscillations of standing water waves are accompanied by a complex of phenomena, as shown in Fig. 1.

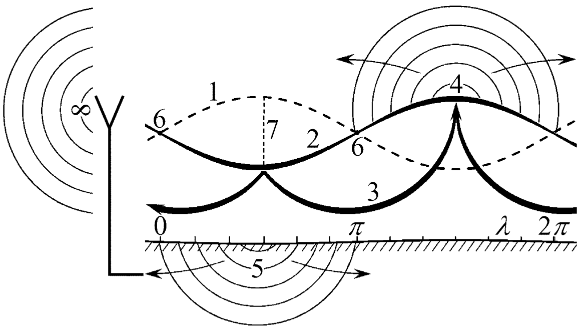


**Figure 1:** A set of phenomena arising from the action of standing water waves in the atmosphere, hydrosphere, and earth's crust (modified from [4])

Abbreviations in Fig. 1: 1–2 are wave amplitude at times $t = 0$, $t = \pi$, respectively; 3 is flow direction just before the wave reaches the optimum value ($t \to \pi$); 4–5, 8 are microbiomes (μb), microseisms (μs) and electromagnetic waves (se) excited by microseismic oscillations at time $t \to \pi$; 6–7 are wave nodes and void spaces. The time t and distance x are measured in conventional units corresponding to the periods of standing wave oscillations $T_{sw}$ and their lengths $\lambda_{sw}$, respectively.

The wave pressure ($p$) in the void at the interface (water and soil for microseismic events, water and air for microbursts) is proportional to the wave amplitude on the water. It can be calculated by the following formulas [12]:

$$\begin{cases} p_{\mu s} = 2\rho_w A^2 \omega^2 \cos(2\omega t); \\ p_{\mu b} = 2\rho_a A^2 \omega^2 \cos(2\omega t) \end{cases} \quad (1)$$

where $\rho$ is the density of water ($\rho_w \approx 1\,000$ kg/m$^3$) for microseismic events and the density of air ($\rho_a \approx 1{,}293$ kg/m$^3$) for microbursts; $A$ is the amplitude of the standing wave; $\omega$ is the cyclic frequency ($\omega = 2\pi/T$); $T$ is the wave period; $t$ is a time variable.

The pressure of a microseismic wave at a distance x from some initial pressure point is defined as [13–14]:

$$p(x)_{\mu s} = p_0 \exp(-\eta_{\mu s} x) \quad (2)$$

Analogously, the pressure of a sound wave at a distance x from some initial pressure point is defined as [15–16]:

$$p(x)_{\mu b} = p_0 \exp(-\eta_{\mu b} x) \quad (3)$$

where $p_0$ is the wave pressure in the source of oscillations; $\eta = h/T$ is the absorption coefficient; $h$ is the attenuation coefficient; $x$ is the distance.

Following the form of joint representation of microseisms and microbars that we have introduced, we write Eqs. 2 and 3 in the form of a system of equations:

$$\begin{cases} p(x)_{\mu s} = p_0 \exp(-\eta_{\mu s} x); \\ p(x)_{\mu b} = p_0 \exp(-\eta_{\mu b} x) \end{cases} \quad (4)$$

The study of geophysical processes shows that the action and development of some phenomena always create prerequisites for the emergence and development of others. The analysis of variations in electromagnetic radiation of the geological environment has shown that they are determined by the mechanisms of energy conversion of these processes, in particular microseismic oscillations, into the energy of the electromagnetic field [1].

There is a good correlation between such phenomena as microseisms and geomagnetic activity [17]. The geomagnetic field, in particular, is affected by microseisms caused by the coupling between ocean waves and the seabed [18]. The locations and time intervals of storm microseisms in 1980 coincided with radio communication disruptions on the international radio relay lines New York—Lüchow (Germany), Lüchow—Tokyo, and Lüchow—Canberra [3].

As a result of the pressure of the water basin's standing waves on the upper layers of the lithosphere, deformations occur due to the slow descending/rising of the earth's surface and vibrations. Deformations result in changes in the pore pressure of groundwater (see Table 1).

In turn, the mechanisms of converting mechanical pressure energy into electromagnetic field energy cause variations in the electromagnetic field of the atmosphere. The complex geophysical fields and processes, and mechanical and electrical transformations cause changes in the geophysical situation of the local environment of the water body in the depressed zone (Fig. 2).

**Table 1**
Mechanisms for converting the energy of geophysical processes into electromagnetic field energy [1]

| Mechanical and electrical converters | Geophysical processes | |
|---|---|---|
| | Deformations due to descending/rising of the Earth's Crust and vibrations | Changing the pore pressure of the groundwater |
| Electrokinetic effect | + | + |
| Electromagnetic induction | + | + |
| Piezo effect | + | – |

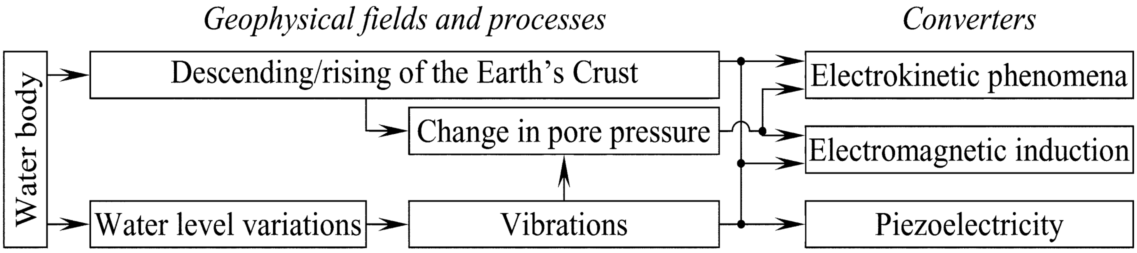


**Figure 2:** Changes in the geophysical situation of the local environment of the water body due to geophysical fields and processes in it, mechanical and electrical transformations [1]

The functional dependence of the electromagnetic wave Ase excited by microseismic oscillations is written as follows:

$$A(x)_{se} = f\left[A(x)_{\mu s}\right] \qquad (5)$$

where f—symbol of a function.

Considering that the simultaneous analysis of infrasound, microseismic, and electromagnetic signals gives sufficiently reliable results, we write the probability of reception in the following form:

$$P_{res} = 1 - \prod_i (1 - P_i),\ i = 3, \qquad (6)$$

where $P_{res}$ is the resulting probability of receiving a hybrid information signal that has more than one manifestation; $P_i$ is the probability of receiving the $i^{th}$ separate signal, which has its transmission medium and physical nature; $i$ is the number of manifestations of the hybrid signal, which are determined by the signal transmission medium, taking into account their physical nature (microbaromes and electromagnetic signal in the atmosphere, microseisms in the lithosphere) [19].

The research method has identified the main variables that are taken into account in the analysis of standing wave oscillations. These are amplitude *A* and attenuation coefficient *h*, period *T*.

## 2.1. Oscillation Amplitudes and Availability of Water Bodies

Natural fluctuations are a general indicator of the existence of any reservoir at any time. If they are not always noticeable, it is only a consequence of the small amplitudes of oscillations in most cases. For example, the height of seiches observed in the plain Kakhovka reservoir before June 6, 2023, the date of the dam's explosion, was 0,02–0,1 m [20]. Longitudinal single-node seiches observed in the Kakhovka reservoir in the summer months of 1970 were active for t1 = 7% of the time, two-node seiches t2 = 11, three-node seiches t3 = 23%, four-node seiches t4 = 2%, five-node seiches t5 = 1%; in the summer months of 1971—t1 = 7%, t2 = 21%, t3 = 29%, t4 = 1%, t5 = 3% [21].

In many reservoirs, seiche is active for 30–50% of the ice-free period. In Lake Baikal, the seiche is almost continuously active, with the highest frequency of single-node oscillations—t1 = 84%; in Lake Balkhash, the seiche is active on average about 60% of the time, in some months the total time of its activity reaches 80% [21].

## 2.2. Oscillation Damping and Oscillation Propagation Range

Due to the inverse proportionality of the absorption coefficient to the period, the low attenuation of long-period oscillations is determined. This applies to both seismic signals (e.g. [3, 7, 14]) and acoustic signals (e.g. [7, 22–23]). Table 2 shows examples of observations of seismic, acoustic, and electromagnetic signals from remote stations.

**Table 2**
Observations of microseismic events (μs), microbursts (μb), magnetic storms (geomagnetic storm—gs) from remote stations

| Source of fluctuations, date of observations | Station (physical nature of the signal) | Distance, km | Amplitude, nm | Period, s |
|---|---|---|---|---|
| Caspian Sea, October 15, 1956 [3] | Makhachkala, Dagestan, Russia (*μs*) | 100 | 9,000 | 3.5 |
| | Baku, Azerbaijan (*μs*) | 320 | 2,000 | 3.4 |
| | Serdar, Turkmenistan (*μs*) | 600 | 600 | 3.2 |
| Indian Ocean, July 1–7, 1957 [3] | Perth, Western Australia (*μs*) | — | 11,000 | 8.0 |
| | Irkutsk magnetic observatory (*gs*) | ≈9,000 | — | 8.0 |
| Indian Ocean, August 16–19, 1958 [3] | Perth, Western Australia; Brisbane, Riverview, Eastern Australia (*μs*) | — | — | 7.0 |
| | Irkutsk magnetic observatory (*gs*) | ≈9,000 | — | 7.0 |
| Indian Ocean, September 22, 1957 [3] | Perth, Western Australia (*μs*) | 3,000 | 5,500 | 8.0 |
| | Irkutsk, Russia (*μs*) | 11,000 | 700 | 8.0 |
| | Irkutsk magnetic observatory (*gs*) | ≈9,000 | — | 8.0 |
| Indian Ocean, September 2, 1958 [3] | Perth, Western Australia; Brisbane, Riverview, Eastern Australia (*μs*) | — | 10,000 | 8.0 |
| | Irkutsk magnetic observatory (*gs*) | ≈9,000 | — | 8.0 |
| Sea of Okhotsk, October 29, 1965 [3] | Petropavlovsk-Kamchatskiy, Russia (*μs*) | 650 | 2,000 | 4.5 |
| | Magadan, Russia (*μs*) | 200 | 2,000 | 5.0 |
| | Tiksi, Sakha, Russia (*μs*) | 2,000 | 200 | 5.0 |
| Lake Baikal, August 20, 1967 [3] | Kabansk, Buryatia, Russia (*μs*) | 50 | 3,000 | 2.8 |
| | Zakamensk, Russia (*μs*) | 200 | 40 | 2,8 |
| | Arshan, Buryatia, Russia (*μs*) | 150 | 100 | 2.5 |
| | Kyakhta, Buryatia, Russia (*μs*) | 200 | 110 | 2.5 |
| Atlantic Ocean, March 17, 1968 [3] | Pulkovo, Russia (*μs*) | 1,890 | 3,500 | 8.6 |
| | Apatity, Murmansk Oblast, Russia (*μs*) | 1,940 | 2,800 | 8.0 |
| | Chișinău, Moldova (*μs*) | 2,800 | 1,400 | 9.0 |
| | Yekaterinburg, Russia (*μs*) | 3,550 | 2,000 | 9.0 |
| | Andijan, Uzbekistan (*μs*) | 5,400 | 500 | 9.0 |
| Earthquake in the Scotia Sea (M = 7.6), August 4, 2003 [24] | Ukrainian Vernadsky Research Base (*μb*) | 1,800 | — | — |
| Barents Sea, October 21–23, 2008 [25] | AS057-Borovoye, Kazakhstan (*μb*) | >2,000 | — | 6–7 |
| | Akbulak, Orenburg Oblast, Russia (*μb*) | >2,000 | — | 6–7 |
| | IS31-Aktyubinsk, Kazakhstan (*μb*) | >2,000 | — | 6–7 |
| Stromboli Volcano at its activity, July 3, August 28, 2019 [7] | Italian National Seismic Network (*μs*) | ~100 | — | — |
| | Italian National Seismic Network (*μb*) | <3,700 | — | — |
| Undermining Kakhovskaya HPS, June 6, 2023, at 2:35 a.m. and 2:54 a.m. | Regional seismic stations from Romania and Ukraine (*μs*) [26] | ≈500–600 | — | — |
| | R1.IBH4—Bucovina, Romania (μb) [27] | <900 | — | — |

### 2.3. Oscillation Periods

An interesting feature of reservoirs is the correspondence of their morphometric characteristics to the period of their oscillations. According to the modified Marian formula for a hypothetical rectangular reservoir of constant depth (with a horizontal bottom), the periods of standing waves in a limited three-dimensional space of the reservoir are determined by its linear dimensions [28]:

$$T = \frac{2}{\sqrt{g\bar{D}}} \times \sqrt{\left(\frac{\bar{L}}{l}\right)^2 + \left(\frac{\bar{W}}{w}\right)^2 + \left(\frac{\bar{D}}{d}\right)^2} \quad (7)$$

where $g$ is the acceleration of free fall ($g$ = 9.81 m/s$^2$); $l$, $w$, and $d$ are indices denoting the number of field half-waves laid along the sides of the reservoirs (length $L$, width $W$, depth $D$, respectively).

According to the available data, the range of periods of natural oscillations (seiches and surf beats) is from 30 seconds to 24 hours.

## 3. Conclusions

The seismic-acoustic method of studying the geophysical situation in the depression zone of a hydroelectric power station reservoir is modified by supplementing the hybrid seismic-acoustic signal with electromagnetic waves excited by microseismic oscillations. The study precedes the development of recommendations for the protection of telecommunications.

The main variables taken into account in the analysis of standing wave oscillations are considered: oscillation amplitude and its attenuation, period.

A generalized hybrid study of natural phenomena and anthropogenic events is reduced to the measurement and subsequent analysis of a hybrid signal that has more than one manifestation. Manifestations are determined by the number of signal transmission media, taking into account their physical nature.

## References


[1] P. Anakhov, et al., (2023). Increasing Functional Stability of Telecommunications Network in the Depressed Zone of HPS Reservoir, Emerging Networking in the Digital Transformation Age (2022) 214–230. doi: 10.1007/978-3-031-24963-1_12.

[2] P. Anakhov, et al., Increasing the Functional Network Stability in the Depression Zone of the Hydroelectric Power Station Reservoir, in: Workshop on Emerging Technology Trends on the Smart Industry and the Internet of Things, vol. 3149 (2022) 169–176.

[3] V. Tabulevich, Comprehensive Studies of Microseismic Oscillations, Novosibirsk: Nauka (1986).

[4] P. Anakhov, Prospects for the Use of Microseisms, Caused by Standing Waves of Water Bodies, Geodynamics 2(33) (2022) 91–98. doi: 10.23939/jgd2022.02.091.

[5] S. Arrowsmith, et al., The Seismoacoustic Wavefield: a New Paradigm in Studying Geophysical Phenomena, Reviews of Geophysics, 48(4) (2010). doi: 10.1029/2010RG000335.

[6] I. Bondar, et al., Central and Eastern European Infrasound Network: Contribution to Infrasound Monitoring, Geophysical J. Int. 230(1) (2022) 565–579. doi: 10.1093/gji/ggac066.

[7] A. Le Pichon, et al., Using Dense Seismo-Acoustic Network to Provide Timely Warning of the 2019 Paroxysmal Stromboli Eruptions, Scientific Reports 11 (2021) 1–12. doi: 10.1038/s41598-021-93942-x.

[8] G. Belli, et al., Infrasonic and Seismic Analysis of Debris-Flow Events at Illgraben (Switzerland): Relating Signal Features to Flow Parameters and the Seismo-Acoustic Source Mechanism, J. Geophysical Res. Earth Surface 127, (2022). doi: 10.1029/2021JF006576.

[9] C. Czanik, et al., Identification of Quarry Blasts Aided by Infrasound Data, Pure and Applied Geophysics 178(6) (2021) 2287–2300. doi: 10.1007/s00024-021-02748-5.

[10] V. Zhebka, et al., Optimization of Machine Learning Method to Improve the Management Efficiency of Heterogeneous Telecommunication Network, in: Workshop on Cybersecurity Providing in Information and Telecommunication Systems, vol. 3288 (2022) 149–155.

[11] V. Zhebka, et al., Stability Method of Connectivity Automated Calculation for Heterogeneous Telecommunication Network, in: Workshop on Cybersecurity Providing in Information and Telecommunication Systems, vol. 3188 (2021) 282–287.

[12] L. Evers, The Inaudible Symphony: on the Detection and Source Identification of Atmospheric Infrasound, Delft University of Technology, Nederland (2008).

[13] J. Wu, et al., (2022). Attenuation Characteristics of Impact-Induced Seismic Wave in Deep Tunnels: An in Situ Investigation Based on Pendulum Impact Test, J. Rock Mechanics Geotechnical Eng. 14(2) 494–504. doi: 10.1016/j.jrmge.2021.12.005.

[14] M. Ogiso, A Method for Mapping Intrinsic Attenuation Factors and Scattering Coefficients of S Waves in 3-D Space and its Application in Southwestern Japan, Geophysical J. Int. 216(2) (2019) 948–957. doi: 10.1093/gji/ggy468.

[15] R. Kapoor, et al., Acoustic Sensors for Air and Surface Navigation Applications, Sensors 18(2) (2018). doi: 10.3390/s18020499.

[16] P. Morse, K. Ingard, Theoretical Acoustics, New York: McGraw-Hill (1968).

[17] J. Laštovička, Relationship Between Microseisms, Geomagnetic Activity and Ionospheric Absorption of Radio Waves, Studia Geophysica et Geodaetica 18(3) (1974) 307–309. doi: 10.1007/BF01624 481.

[18] C. Chieh-Hung, et al., Magnetic Pulsations Triggered by Microseismic Ground Motion, J. Geophysical Res. Solid Earth 126(3) (2021). doi: 10.1029/2020JB021416.

[19] P. Anakhov, et al., Evaluation Method of the Physical Compatibility of Equipment in a Hybrid Information Transmission Network, Journal of Theoretical and Applied Information Technology 100(22) (2022) 6635–6644.

[20] N. Labzovsky, Noncyclic Sea Level Fluctuations, Gidrometeoizdat, Leningrad (1971).

[21] A. Sudol'skij, Dynamic Phenomena in Reservoirs, Gidrometeoizdat, Leningrad (1991).

[22] M. De Carlo, F. Ardhuin, A. Le Pichon, Atmospheric Infrasound Generation by Ocean Waves in Finite Depth: Unified Theory and Application to Radiation Patterns, Geophysical J. Int. 221(1) (2020) 569–585. doi: 10.1093/gji/ggaa 015.

[23] J. Bowman, G. Baker, M. Bahavar, Ambient Infrasound Noise, Geophysical Res. Letters 32(9) (2005). doi: 10.1029/2005GL022486.

[24] O. Lyashchuk, E. Karyagin, Monitoring of Unsafe Man-Made and Natural Phenomena in the Infrasonic Range, Acoustic Symposium "Consonance-2013," Institute of Hydromechanics of the National Academy of Sciences of Ukraine, Kyiv (2013) 188–193.

[25] V. Dubrovin, A. Smirnov, Recording Andparametrization of Microseism and Microbaromsusing Data of NNC RK Monitoring Network, National Nuclear Center of the Republic of Kazakhstan Bulletin (2) (2009) 172–178.

[26] NORSAR, Seismic Signals Recorded from an Explosion at the Kakhovka Dam in Ukraine June 6th, 2023 (2023). URL: https://www.norsar.no/in-focus/seismic-signals-recorded-from-an-explosion-at-the-kakhovka-dam-in-ukraine

[27] N. Lazur, Not Self-Destruction and Not Flying: a Physicist Recorded Evidence that the Kakhovskaya HPP Was Blown Up (2023). URL: https://24tv.ua/pidriv-kahovskoyi-ges-6-chervnya-2023-fizik-pidtverdiv-shho-yiyi_n2329441

[28] P. Anakhov, Three-Dimentional Model of the Deformation of Structural Merian Basin by Standing Waves, Geodynamics 2(27) (2019) 48–53. doi: 10.23939/jgd2019.02.048.